

000
001
002
003
004
005
006
007
008
009
010
011
012
013
014
015
016
017
018
019
020
021
022
023
024
025
026
027
028
029
030
031
032
033
034
035
036
037
038
039
040
041
042
043
044
045
046
047
048
049
050
051
052
053

EMBEDDING-BASED CONTEXT-AWARE RERANKER

Anonymous authors

Paper under double-blind review

ABSTRACT

Retrieval-Augmented Generation (RAG) systems rely on retrieving relevant evidence from a corpus to support downstream generation. The common practice of splitting a long document into multiple shorter passages enables finer-grained and targeted information retrieval. However, it also introduces challenges when a correct retrieval would require inference across passages, such as resolving coreference, disambiguating entities, and aggregating evidence scattered across multiple sources. Many state-of-the-art (SOTA) reranking methods, despite utilizing powerful large pretrained language models with potentially high inference costs, still neglect the aforementioned challenges. Therefore, we propose *Embedding-Based Context-Aware Reranker (EBCAR)*, a lightweight reranking framework operating directly on embeddings of retrieved passages with enhanced cross-passage understandings through the structural information of the passages and a hybrid attention mechanism, which captures both high-level interactions across documents and low-level relationships within each document. We evaluate EBCAR against SOTA rerankers on the ConTEB benchmark, demonstrating its effectiveness for information retrieval requiring cross-passage inference and its advantages in both accuracy and efficiency.

1 INTRODUCTION

Retrieval-Augmented Generation (RAG) systems (Lewis et al., 2020; Wu et al., 2024) have become a cornerstone for enabling language models to incorporate external knowledge in complex reasoning tasks such as question answering (Mao et al., 2021; Xu et al., 2024b), fact verification (Adjali, 2024; Yue et al., 2024), and dialogue generation (Huang et al., 2023; Wang et al., 2024a). A typical RAG pipeline consists of a retriever, identifying relevant passages from a large corpus, and a reranker, reordering these candidates to surface the most useful evidence for downstream generation. The reranker plays a critical role in filtering out noisy retrieval results and promoting passages that are more faithful, complete, and relevant to the input query (Glass et al., 2022; de Souza P. Moreira et al., 2024). To support fine-grained retrieval, modern pipelines often rely on passage-level indexing, where a long document is split into shorter fixed-size passages for retrieval. This chunking process refines the granularity of retrieval and improves the readability of retrieved content for downstream models (Xu et al., 2024a; Jiang et al., 2024). While long-context encoders and embedding models have recently emerged (Zhang et al., 2024; Warner et al., 2024; Boizard et al., 2025; Zhu et al., 2024), passage-level retrieval remains the dominant design choice in many deployed systems due to its effectiveness and efficiency (Wu et al., 2024; Conti et al., 2025).

Existing reranking methods typically fall into three paradigms (Sharifymoghaddam et al., 2025): **(i)** Pointwise scoring models evaluate each query-passage pair independently. For example, Nogueira et al. (2019) and Nogueira et al. (2020) score individual query-passage pairs using pretrained language models (PLMs), by formulating the task as a binary classification problem or as a generative task requiring a “True” or “False” token as the output. **(ii)** Pairwise approaches compare pairs of passages to infer relative relevance; for instance, Pradeep et al. (2021) estimates the probability that one passage is more relevant than another given the query. **(iii)** Listwise methods, in contrast, operate over the entire set of retrieved candidates at once. One common practice is to prompt large language models (LLMs) to directly output a reranked list (Sun et al., 2023). Another is to distill supervision signals from LLMs into smaller generative models (Pradeep et al., 2023a;b; Gangi Reddy et al., 2024). Recently, inference-time methods have been proposed that prompt an LLM to compute calibrated attention-based scores across the retrieved passages (Chen et al., 2025).

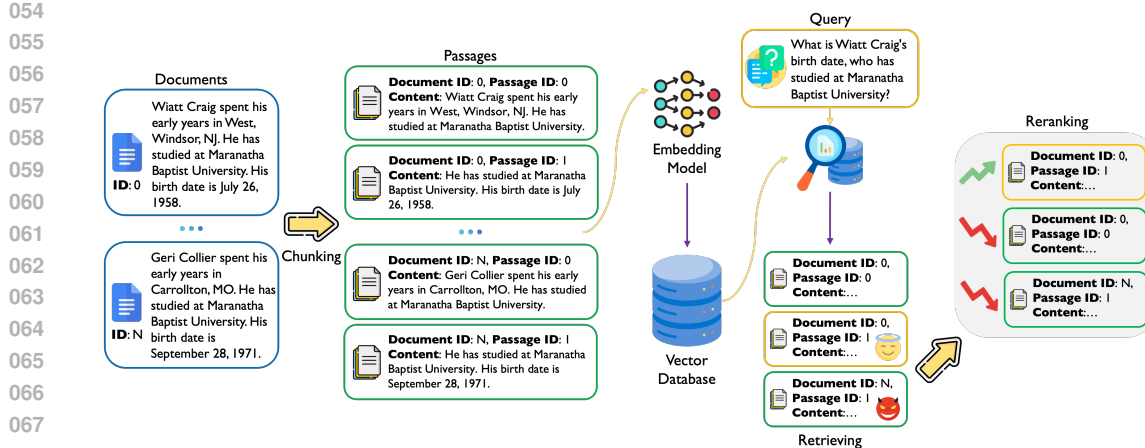


Figure 1: A Retrieval-Augmented Generation (RAG) pipeline with passage-level retrieval. Long documents are chunked into passages before being embedded into a dense vector store. At query time, top- k passages are retrieved and reranked to provide evidence for downstream generation.

Despite recent progress, two important challenges in reranking remain underexplored. First, across pointwise, pairwise, and listwise paradigms, most rerankers rely on feeding the raw text of retrieved passages and the query into large pretrained language models (PLMs) for scoring. This strategy incurs substantial computational cost and latency during inference, making it less practical for real-world deployments. Second, many existing methods are evaluated on idealized benchmarks that assume the necessary information for answering a query is fully contained within a single passage, leaving the capabilities of current reranking strategies underexplored in scenarios that demand cross-passage inference (Conti et al., 2025; Thakur et al., 2025; Zhou et al., 2025). As illustrated in Figure 1, consider the query “What is Wiatt Craig’s birth date, who has studied at Maranatha Baptist University?” Passages related to “Wiatt Craig”, “birth date”, and “Maranatha Baptist University” may all be retrieved individually. However, multiple retrieved passages mention the birth date of a person who studied at Maranatha Baptist University, but without resolving the pronoun “he”, the reranker cannot determine which passage truly pertains to “Wiatt Craig”, leading to misranking.

To address the dual challenges of inference inefficiency and insufficient modeling of cross-passage context, we propose *Embedding-Based Context-Aware Reranker (EBCAR)*. In contrast to prior rerankers that rely on scoring raw text using large PLMs, EBCAR operates directly on the dense embeddings of queries and retrieved passages. These passage embeddings are readily available, as they are stored in a vector database during indexing. The query embedding is obtained at inference time using the same encoder employed during passage indexing, ensuring compatibility in representation space. This design decouples reranking from costly text-to-text inference, substantially improving computational efficiency and enabling low-latency deployment. To facilitate cross-passage inference, EBCAR incorporates structural signals, such as document IDs and the positions of passages within their original documents, via positional encodings. These encodings are processed by a transformer encoder equipped with a *hybrid attention mechanism*, comprising two complementary multi-head attention modules: a *shared full attention* module and a *dedicated masked attention* module. Both modules operate on the same input representations but differ in their attention scopes. The shared full attention allows the query and all passage embeddings to attend to one another, capturing global interactions across retrieved passages. In contrast, the dedicated masked attention restricts attention scopes to the passages originating from the same documents, as determined by their document IDs. This hybrid attention design enables the model to infer over both inter-document context and fine-grained intra-document dependencies, promoting more accurate evidence aggregation and entity disambiguation. We evaluate EBCAR on ConTEB (Conti et al., 2025), a challenging benchmark originally designed to test retrieval models’ use of document-wide context but used in our work to assess rerankers. Our experiments include both in-distribution evaluations and out-of-distribution zero-shot tests on entirely unseen domains, where EBCAR achieves promising performance.

Our main contributions are summarized as follows:

- We highlight the challenges of both efficiency and cross-passage inference in reranking, and introduce a lightweight embedding-based framework to address them.

- 108 • We propose a hybrid attention architecture that incorporates structural signals, such as doc-
109 ument identity and passage position, through positional encodings, and combines shared
110 full and dedicated masked attention modules to enhance context-aware reranking.
- 111 • We conduct extensive evaluations on ConTEB, demonstrating that EBCAR achieves
112 promising performance in both in-distribution and out-of-distribution zero-shot settings,
113 with significantly lower inference latency.

115 2 RELATED WORK

118 In this section, we review prior work related to reranking from three perspectives: existing context-
119 aware methods to enhance retrieval systems, the design of reranking methods, and the evaluation
120 protocols used to assess their capabilities.

122 **Contextual Retrieval.** Prior work has proposed several methods to enhance retrieval systems with
123 broader contextual understanding beyond isolated passages. For instance, late chunking (Günther
124 et al., 2025), semantic chunking (Qu et al., 2024), and hierarchical retrieval (Arivazhagan et al.,
125 2023; Choe et al., 2025) aim to improve retrieval granularity by better aligning the unit of retrieval
126 with semantic boundaries or document structure. These methods operate at the retrieval or genera-
127 tion stage and have proven effective in enhancing RAG pipelines. In contrast, our work focuses
128 on the reranking stage and introduces architectural mechanisms to explicitly model intra and inter-
129 passage dependencies within the reranker. We position EBCAR as complementary to the above
130 techniques: it can be integrated seamlessly into RAG pipelines that already incorporate context-
131 aware retrieval or generation strategies, providing an additional layer of cross-passage inference
132 during candidate reranking.

133 **Reranking Methods.** Existing reranking approaches can be broadly categorized into three
134 paradigms: pointwise, pairwise, and listwise. **(i)** Pointwise models treat reranking as a binary classi-
135 fication or regression task and score each query–passage pair independently. MonoBERT (Nogueira
136 et al., 2019) formulates reranking as a binary classification problem using BERT to predict whether
137 a passage is relevant to a given query. MonoT5 (Nogueira et al., 2020) adopts a generative approach,
138 fine-tuning a T5 model to generate the tokens “True” or “False” and computing the predicted rel-
139 evance score via softmax over the logits of these two tokens. However, pointwise rerankers incur
140 high inference costs, as they require a separate forward pass for each candidate passage.

141 **(ii)** Pairwise methods compare two candidate passages at a time to infer their relative relevance to
142 the query. DuoT5 (Pradeep et al., 2021), for instance, estimates the probability that one passage
143 is more relevant than another. The resulting pairwise orders are typically aggregated, using sorting
144 heuristics or tournament-based voting, to yield a final ranking. While pairwise approaches can better
145 capture comparative relevance than pointwise methods, their computational cost grows quadratically
146 with the number of candidates.

147 **(iii)** Listwise methods score or reorder the entire set of retrieved passages jointly. While earlier
148 methods treated this holistically using traditional architectures, most recent listwise approaches
149 leverage large language models (LLMs) in different ways, leading to three main subcategories in
150 practice. *Prompt-only reranking* directly queries a powerful LLM, e.g., GPT-3.5 or GPT-4, to re-
151 turn a ranked list of passages in a single forward pass. For example, RankGPT (Sun et al., 2023)
152 prompts the model to reorder passages based on their relevance to the query. While effective in
153 zero-shot settings, this approach depends on proprietary APIs and incurs high inference latency and
154 computational cost. *LLM-supervised distillation* extracts listwise supervision signals from prompt-
155 only LLMs and uses them to fine-tune smaller, open-source models. RankVicuna (Pradeep et al.,
156 2023a), RankZephyr (Pradeep et al., 2023b), and Lit5Distill (Tamber et al., 2023) fine-tune 7B-scale
157 or smaller models using the ranked outputs from GPT-style models. Similarly, FIRST (Gangi Reddy
158 et al., 2024) and FIRST-Mistral (Chen et al., 2024) use the logits of the first generated token as a
159 ranking signal, while PE-rank (Liu et al., 2025) compresses passage context into a single embedding
160 for efficient listwise reranking. These distilled models preserve much of the performance of larger
161 LLMs while offering improved inference efficiency. *Inference-time relevance extraction* bypasses
162 generation entirely by computing relevance scores from internal attention or representation patterns
163 of LLMs. ICR (Chen et al., 2025), for instance, derives passage-level relevance using attention-

162 based signals from a calibration prompt and two forward passes through the LLM. While more
 163 efficient, these methods still rely on large models and full-text processing during inference.
 164

165 **Evaluation Settings.** Most existing rerankers are trained on the MS-MARCO passage ranking
 166 dataset (Bajaj et al., 2016) and evaluated in a zero-shot manner on benchmarks such as the TREC
 167 Deep Learning (DL) tracks (Craswell et al., 2020; 2021) and the BEIR benchmark suite (Thakur
 168 et al., 2021). While these datasets have driven substantial progress, they predominantly feature self-
 169 contained passages that independently provide sufficient information to answer a query. This design
 170 simplifies the reranking task and limits the need for inference across multiple passages or lever-
 171 aging broader document-level context (Conti et al., 2025; Thakur et al., 2025). In addition, struc-
 172 tural signals such as document identifiers or passage positions are often absent or unused in these
 173 benchmarks. To address these limitations, we evaluate our proposed EBCAR on ConTEB (Conti
 174 et al., 2025), a benchmark originally developed to assess retrievers’ use of document-wide context,
 175 which we use as a challenging testbed to evaluate rerankers’ ability to infer across multiple retrieved
 176 passages in both in-distribution and out-of-distribution scenarios. In this work, we use the term
 177 *cross-passage inference* to broadly refer to settings where relevant information is distributed across
 178 multiple passages, requiring models to aggregate and reconcile evidence across them.
 179

180 3 METHODOLOGY

181 Rerankers aim to refine a list of candidate passages retrieved for a query, producing a final rank-
 182 ing that better reflects passage relevance. In this work, we propose an embedding-based rerank-
 183 ing framework that jointly scores candidate passages while leveraging cross-passage context and
 184 document-level structure. Our approach operates entirely in the embedding space, enabling fast and
 185 scalable inference. Below, we formally define the embedding-based reranking problem and present
 186 our proposed method in detail.
 187

188 3.1 EMBEDDING-BASED FRAMEWORK

189 Given a user-issued query x_q and a set of candidate passages $\{x_1, x_2, \dots, x_k\}$ retrieved from a vec-
 190 tor store, the goal is to reorder them based on their contextual relevance to the query. Each passage
 191 x_i is associated with a pre-computed embedding $p_i \in \mathbb{R}^d$, obtained during indexing via a shared
 192 embedding function $\mathcal{E}(\cdot)$, i.e., $p_i = \mathcal{E}(x_i)$. These passage embeddings remain fixed during infer-
 193 ence, and only the query needs to be encoded as $q = \mathcal{E}(x_q)$ using the same embedding function. The
 194 reranker aims to produce a permutation $\pi(\cdot)$ over the indices $\{1, 2, \dots, k\}$ such that the reordered
 195 list $\{x_{\pi(1)}, \dots, x_{\pi(k)}\}$ places the most relevant passages to q at the top. This formulation enables
 196 efficient and parallelizable inference over dense embeddings.
 197

198 3.2 EMBEDDING-BASED CONTEXT-AWARE RERANKER

199 **Architecture.** To capture both inter-document and intra-document dependencies among candidate
 200 passages, we propose a hybrid-attention-based reranking architecture, EBCAR, that operates on pre-
 201 computed dense embeddings. As shown in Figure 2, EBCAR integrates document identifiers and
 202 passage position information into the encoding process, and leverages a hybrid attention mechanism
 203 to model both global and document-local interactions.
 204

205 We begin by augmenting the passage embeddings with structural signals. Given k candidate pas-
 206 sages $\{x_1, \dots, x_k\}$ with corresponding dense embeddings $\{p_1, \dots, p_k\}$, each passage embedding
 207 $p_i \in \mathbb{R}^d$ is enriched with two additional embeddings: a *document ID embedding* $\text{doc}(i) \in \mathbb{R}^d$,
 208 indicating the document to which x_i belongs, and a *passage position encoding* $\text{pos}(i) \in \mathbb{R}^d$,
 209 reflecting the position of x_i within its original document. These components are combined as
 210 $\tilde{p}_i = p_i + \text{doc}(i) + \text{pos}(i)$. The document ID embeddings are only used to distinguish the unique
 211 documents that the current retrieved passages belong to, instead of all the documents in the corpus.
 212 The i -th document ID embedding corresponds to the i -th unique document from the current k re-
 213 trievalled passages. As a result, the document ID embedding table has a maximum size of $k \times d$ and
 214 remains fixed across training and inference. **Importantly, the document ID embeddings are *relative***
 215 **and *local*** to each retrieved candidate set, rather than global corpus-level identifiers. At inference
 time, we re-index document IDs on-the-fly according to the unique source documents within the k

retrieved passages. The document ID embeddings table is reused across all queries and kept *frozen*. For example, suppose the retriever returns $k = 6$ passages for query q , where x_1, x_2, x_4 come from document A, x_3, x_5 from document B, and x_6 from document C. EBCAR dynamically assigns three document IDs for this candidate set, e.g., $\text{doc}(1) = \text{doc}(2) = \text{doc}(4) = \mathbf{e}_1$, $\text{doc}(3) = \text{doc}(5) = \mathbf{e}_2$, $\text{doc}(6) = \mathbf{e}_3$, where $\mathbf{e}_1, \mathbf{e}_2$, and \mathbf{e}_3 are selected from the same fixed-size embedding table. When processing another query q' , the retriever may return a different set of six passages x'_1, \dots, x'_6 from entirely different documents, e.g., A', B', C'; these will again be assigned document embeddings $\mathbf{e}_1, \mathbf{e}_2, \mathbf{e}_3$ from the same table. The primary purpose of this design is to enable the model to learn to recognize which passages originate from the same document through these relative document ID embeddings, thereby facilitating within-document reasoning. As a secondary benefit, this dynamic formulation also allows new documents to be incorporated without retraining: each new document is simply assigned a temporary local document ID during reranking. The passage position encodings follow a standard sinusoidal design. The query embedding $q \in \mathbb{R}^d$ remains unchanged. We concatenate the query with the enriched passage embeddings along the sequence length axis to form an input sequence, as shown in Figure 2, which is then processed by a stack of M modified Transformer encoder layers.

Each Transformer encoder layer employs a hybrid attention mechanism composed of two modules. The *shared full attention* module is a standard multi-head attention mechanism that allows the query and all passages to attend to one another freely, capturing global relevance and inter-document relationships. In contrast, the *dedicated masked attention* module restricts each passage's attention to only those passages within the same document, plus the query, enabling fine-grained modeling of intra-document coherence. Formally, the attention score of this module is computed as:

$$\text{DedicatedAttnScore}(Q, K) = \text{softmax} \left(\frac{QK^\top + \text{mask}_{\text{doc}}}{\sqrt{d_k}} \right), \quad (1)$$

where Q and K are the query and key matrices, respectively, and d_k is the head dimension. The additive attention mask $\text{mask}_{\text{doc}} \in \mathbb{R}^{(k+1) \times (k+1)}$ is defined such that the (i, j) -th entry is 0 if passage j belongs to the same document as passage i or if j is the query embedding, and $-\infty$ otherwise. This masking encourages the model to reason locally within documents without interference from unrelated passages. As illustrated in Figure 2, this masking pattern ensures that: (i) the query can attend to all passages, (ii) passage p_1 from, e.g., document 0 can attend to the query and passage p_2 from the same document, but not to p_3 from, e.g., document N , and (iii) passage p_3 from document N can attend only to the query and itself. Note that the dedicated attention mechanism always allows each passage to attend to the query, ensuring that the model can implicitly recognize the query position as special without any additional signals. To better illustrate how the two attention modules complement each other, consider the example below.

Query: When did Hull City win the 2016 Championship play-off final?

Retrieved passages (p_1, p_2 **are from Document A;** p_3, p_4 **are from Document B):**

p_1 : Hull City is a professional football club based in Kingston upon Hull, England.

p_2 : They reached the 2016 Championship play-off final after finishing fourth in the league.

p_3 : The Championship play-off final determines which team is promoted to the Premier League.

p_4 : This match of 2016 took place on 28 May at Wembley Stadium.

Within each document, the *dedicated masked attention* facilitates local reasoning, linking "They" to "Hull City" in Document A, and connecting "This match" to "the Championship play-off final" in Document B. Across documents, the *shared full attention* enables global interaction, aligning the "Hull City" in Document A with the event context in Document B to identify that passage p_4 contains the answer. Together, the two modules complement each other: the *dedicated masked attention* consolidates intra-document coherence, while the *shared full attention* integrates evidence across documents for accurate cross-passage reasoning. The outputs of the two modules are summed and passed through a feedforward network with residual connections and layer normalization. After M stacked layers, we extract the updated passage embeddings $\{\hat{p}_1, \dots, \hat{p}_k\}$ from the output sequence. These contextualized embeddings are then used to compute the final relevance scores.

Training Objective. Given a query q and a set of candidate passages $\{x_1, \dots, x_k\}$, each passage is labeled as either positive or negative based on its relevance to the query. Let $q \in \mathbb{R}^d$ denote the original query embedding, and $\{\hat{p}_1, \dots, \hat{p}_k\}$, the updated passage embeddings obtained from the

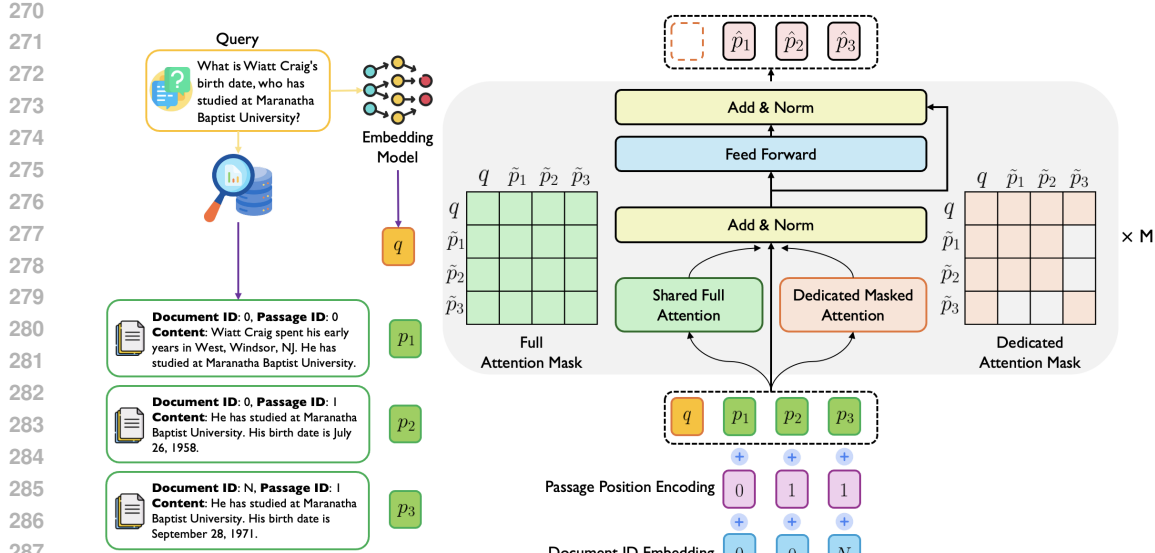


Figure 2: Overview of the EBCAR architecture. Candidate passage embeddings are enriched with document ID and passage position information, then processed jointly with the query embedding through a Transformer encoder. The hybrid attention mechanism combines a shared full attention module and a **dedicated masked** attention module. **The outputs of the two modules are summed with residual connections and layer normalization.**

final Transformer encoder layer in EBCAR. Our training objective encourages the updated representation of the positive passage to be close to the query embedding, while pushing the negatives away. Therefore, we adopt a contrastive learning objective based on dot-product similarity and employ the InfoNCE loss (van den Oord et al., 2018) defined as:

$$\mathcal{L}_{\text{contrast}} = -\log \frac{\exp(\text{sim}(q, \hat{p}^+))}{\exp(\text{sim}(q, \hat{p}^+)) + \sum_j \exp(\text{sim}(q, \hat{p}_j^-))}, \quad (2)$$

where \hat{p}^+ is the updated embedding of the positive passage, $\{\hat{p}_j^-\}$ are the embeddings of the negative passages, and $\text{sim}(a, b) = a^\top b$ denotes dot-product similarity.

We intentionally use the unmodified query embedding q , instead of the query's updated embedding, to maintain a consistent reference point across candidate sets. This design choice avoids query-specific drift caused by the passage context and ensures that the passage representations are directly optimized to align with the static semantic anchor of the query. **We validate this design in Appendix A.1, where we compare the training stability between fixed and updated query embeddings.**

Inference. At inference time, we compute the relevance scores between the query and each candidate passage based on their final embeddings. Given the updated passage embeddings $\{\hat{p}_1, \dots, \hat{p}_k\}$ and the static query embedding q , we compute $s_i = \text{sim}(q, \hat{p}_i)$, for $i = 1, \dots, k$. The final passage ranking is obtained by sorting the scores $\{s_1, \dots, s_k\}$ in descending order. This process is efficient and deterministic, leveraging the contextualized passage representations produced by EBCAR.

4 EXPERIMENTS

We conduct comprehensive experiments to evaluate the effectiveness and efficiency of our proposed EBCAR reranker. Our study is designed to answer the following research questions: **Q1**: Does EBCAR achieve competitive or superior performance compared to existing methods on datasets that require cross-passage inference? **Q2**: Is EBCAR more efficient at inference time than existing SOTA rerankers? **Q3**: Are EBCAR's architectural components, namely the passage position encoding and the hybrid attention mechanism, individually beneficial? **Q4**: How does EBCAR perform on datasets that require less cross-passage inference, particularly in out-of-distribution settings? **Q5**: How does

EBCAR perform when the number of retrieved passages scales up? To answer these questions, the remainder of this section is organized as follows: we first describe the datasets and evaluation protocol, followed by a summary of the baseline methods. We then present our main experimental results and provide an analysis of effectiveness and inference efficiency. Finally, we conduct ablation studies. In Appendix A.6 and Appendix A.7, we evaluate the generalization ability of EBCAR on datasets that do not emphasize cross-passage inference and the impact of retrieved candidate size.

4.1 DATASETS AND EVALUATION PROTOCOL

We conduct our evaluation on ConTEB¹ (Conti et al., 2025), a recently introduced benchmark designed to test whether retrieval models can leverage document-wide context when encoding individual passages. We use ConTEB as a challenging testbed for evaluating rerankers’ abilities to perform context-aware reranking with cross-passage inference. Many of the benchmark datasets comprise long documents where relevant information is dispersed across chunks or coreferences and structural cues are essential for resolving ambiguity. Our experiments include both in-distribution evaluations, where test queries originate from the same domains as the training data, and out-of-distribution evaluations, where test queries are drawn from entirely different domains than training.

Training Procedure. We train EBCAR on the ConTEB training splits: MLDR, SQuAD, and NarrativeQA. These datasets emphasize different forms of cross-passage inference, including entity-level disambiguation, fine-grained span matching, and narrative-level context comprehension. The training corpus consists of 311,337 passages and 362,142 training queries. For validation, we randomly sample 2,000 queries from the full set of 21,370 queries provided in the ConTEB validation split. To construct training examples, we use Contriever (Izacard et al., 2021) to retrieve the top-20 passages for each query. Since the gold passage is not guaranteed to appear among the retrieved candidates, we check its presence and, if absent, replace the 20th-ranked passage with the gold-positive one. This ensures that each training instance contains exactly one positive and up to nineteen negative passages. To avoid bias from retrieval rank, we randomly shuffle the passage order within each candidate set before feeding it to the model. It is worth mentioning that during inference and evaluation, we follow the same retrieval pipeline but do not enforce the inclusion of the gold passage; the top-20 candidates are taken directly from Contriever without any oracle intervention.

Test Datasets. We evaluate EBCAR on eight datasets from the ConTEB benchmark, covering both in-distribution and out-of-distribution scenarios. **(i)** MLDR, **(ii)** SQuAD, and **(iii)** NarrativeQA (NarrQA) are used for both training and evaluation, enabling assessment of in-distribution performance for EBCAR and baselines trained on these three datasets. MLDR and NarrativeQA consist of encyclopedic and literary documents, respectively, where relevant information may be scattered across long passages. **(iv)** COVID-QA (COVID) is a biomedical QA dataset based on scientific research documents, which similarly requires reasoning over long and dense texts. **(v)** ESG Reports are long-form corporate documents sourced from the ViDoRe benchmark, re-annotated for text-based QA to test document-wide contextual understanding capabilities. **(vi)** Football and **(vii)** Geography (Geog) are constructed from rephrased Wikipedia summaries in which explicit entity mentions have been replaced by pronouns via GPT-4o. This setup introduces referential ambiguity and demands cross-passage entity disambiguation and coreference resolution to answer correctly. **(viii)** Insurance (Insur) comprises statistical reports on European Union countries, where country names often appear only in section headers, and therefore requires knowledge of a passage’s structural position within the document to disambiguate country-specific information.

Evaluation Metrics. We report nDCG@10 as our main effectiveness metric in Section 4.4, with MRR@10 results provided in Appendix A.2. Both metrics evaluate ranking quality and precision. We additionally measure inference efficiency using throughput, defined as the number of queries processed per second on a single A100 GPU with batch size 1. This dual-axis evaluation allows us to assess each reranker’s practicality in latency-sensitive deployment settings.

4.2 COMPARISON METHODS

We compare EBCAR against baselines spanning four categories: retriever-only, pointwise, pairwise, and listwise rerankers. All methods rerank the same set of 20 candidate passages retrieved by Con-

¹<https://huggingface.co/collections/illuin-conteb/conteb-evaluation-datasets>

378 Table 1: nDCG@10 across datasets. **Orange** denotes in-distribution tests, and **Green** denotes out-
 379 of-distribution tests. Throughput is the number of queries processed per second on a single A100
 380 GPU. The best and second best results are **bolded** and underlined, respectively.
 381

382 Method	383 Training	384 Size	MLDR	SQuAD	NarrQA	COVID	ESG	Football	Geog	Insur	Avg	Throughput
385 BM25	-	-	65.42	45.07	36.20	39.79	10.10	4.69	23.66	0.00	28.12	263.16
386 Contriever	-	-	60.23	54.63	66.97	31.02	15.69	5.95	46.39	2.75	35.45	29.67
387 monoBERT (base)	ConTEB Train	110M	40.44	27.94	36.63	20.52	11.67	4.01	29.23	2.92	21.67	4.24
388 monoT5 (base)	ConTEB Train	223M	26.76	19.75	41.21	24.56	10.37	5.69	36.70	4.40	21.18	1.69
389 monoT5 (base)	MS-MARCO	223M	70.47	67.00	58.89	41.51	18.61	9.68	54.47	2.20	40.37	3.61
390 duoT5 (base)	MS-MARCO	223M	42.34	68.63	21.46	18.19	12.69	8.84	47.18	2.57	27.74	0.18
391 RankVicuna	MS-MARCO	7B	79.30	66.59	79.48	51.87	22.97	11.46	71.08	4.27	48.38	0.17
392 RankZephyr	MS-MARCO	7B	82.34	69.06	81.18	53.15	26.42	11.63	72.91	3.51	50.03	0.17
393 FIRST	MS-MARCO	7B	74.78	61.55	78.62	41.17	20.06	7.88	60.92	3.21	43.52	1.73
394 FirstMistral	MS-MARCO	7B	74.41	62.19	78.69	41.35	20.26	7.78	61.79	3.40	43.73	1.78
395 LiT5Distil	MS-MARCO	248M	60.33	54.87	66.94	31.22	16.07	5.98	46.66	2.78	35.61	0.66
396 PE-Rank	MS-MARCO	8B	52.58	45.00	51.58	33.40	19.92	6.29	46.25	1.37	32.05	0.81
397 RankGPT (Mistral)	-	7B	65.75	56.61	68.29	33.23	15.04	7.67	51.75	3.05	37.67	0.12
398 RankGPT (Llama)	-	8B	76.80	61.16	74.74	47.80	20.49	11.10	71.37	4.76	46.03	0.13
399 ICR (Mistral)	-	7B	79.49	67.41	79.50	52.54	25.65	10.57	71.44	4.00	48.83	0.18
400 ICR (Llama)	-	8B	83.93	69.09	79.96	53.32	28.36	10.91	73.10	4.16	50.35	0.19
401 EBCAR (ours)	ConTEB Train	126M	75.26	71.62	73.21	59.80	37.20	80.19	81.30	40.74	64.92	29.33

398 triever, without any oracle modification. **(a) Retriever-only baselines:** **(i)** BM25 is a classical sparse
 399 retriever based on lexical matching. **(ii)** Contriever (Izacard et al., 2021) is a dense retriever trained
 400 using unsupervised contrastive learning. **(b) Pointwise rerankers:** **(iii)** monoBERT (Nogueira
 401 et al., 2019) independently scores each query–passage pair using a binary classification head. **(iv)**
 402 monoT5 (Nogueira et al., 2020) casts reranking as a text generation task by producing the to-
 403 ken “True” or “False.” **(v)** monoT5 (MS-MARCO) refers to the same model trained on the MS-
 404 MARCO (Bajaj et al., 2016) dataset. **(c) Pairwise rerankers:** **(vi)** duoT5 (Pradeep et al., 2021)
 405 compares passage pairs to estimate their relative preference with respect to the query. **(d) Listwise
 406 rerankers:** **(vii)** RankVicuna (Pradeep et al., 2023a), **(viii)** RankZephyr (Pradeep et al., 2023b), and
 407 **(ix)** LiT5Distill (Tamber et al., 2023) are distilled listwise rerankers supervised by ranked outputs
 408 from GPT-style models. **(x)** FIRST (Gangi Reddy et al., 2024) and **(xi)** FirstMistral (Chen et al.,
 409 2024) use the logits of the first generated token to derive passage-level ranking scores. **(xii)** PE-
 410 Rank (Liu et al., 2025) encodes each passage into a single embedding for efficient listwise ranking.
 411 **(xiii)** RankGPT (Sun et al., 2023) prompts a language model to return a ranked list. **(xiv)** ICR (Chen
 412 et al., 2025) computes passage relevance using attention-based signals from in-context calibrated
 413 prompts over LLM representations. Due to limitations of computational resources, we only train
 414 monoBERT and monoT5 on ConTEB and evaluate other baselines with their provided checkpoints.

415 4.3 IMPLEMENTATION DETAILS

416 For training our EBCAR, we use the Adam optimizer (Kingma & Ba, 2015) with a fixed learning
 417 rate of 1×10^{-3} and no weight decay. The model is trained for up to 20 epochs, with early stopping
 418 based on validation loss using a patience of 5 epochs. We set the batch size to 256. The default
 419 EBCAR configuration uses 16 layers, i.e., $M = 16$, a hidden size of 768, 8 attention heads. We
 420 employ these configurations to obtain similar amount of parameters as BERT base model. The
 421 implementation details of baseline methods are discussed in Appendix A.3. All experiments are run
 422 on a single A100 GPU.

423 4.4 RESULTS AND ANALYSIS

425 **Effectiveness.** We first compare the overall ranking quality of EBCAR with a broad set of base-
 426 lines. As shown in Table 1, EBCAR achieves the highest average nDCG@10 across all test sets,
 427 outperforming all baselines. Our method shows particularly strong gains on tasks that require fine-
 428 grained entity disambiguation and coreference resolution, such as Football and Geography, where
 429 reasoning across multiple passages and resolving entity mentions is essential. EBCAR also excels
 430 on Insurance, a task that heavily relies on positional information and structured document layouts; in
 431 this case, our architecture’s ability to incorporate explicit passage position embeddings proves ben-
 432 efitical. These targeted improvements reflect the strengths of EBCAR in handling tasks that benefit

432 from structured passage representation and alignment. We illustrate one sample from the football
 433 dataset and one from the insurance dataset in Appendix A.4 to highlight the underlying challenges.
 434

435 On the remaining datasets, including both in-distribution datasets like MLDLR, SQuAD, and Narra-
 436 tiveQA, and out-of-distribution datasets such as ESG and COVID, EBCAR maintains competitive
 437 performance. While it does not always surpass the most powerful LLM-based rerankers, e.g., ICR,
 438 we hypothesize that this is partly due to EBCAR’s embedding-based architecture: since each passage
 439 is compressed into a fixed-size embedding, some fine-grained information may be lost, a limitation
 440 not shared by LLM rerankers that directly process the full text of each passage.
 441

442 Despite this potential information bottleneck, EBCAR achieves strong and stable performance
 443 across domains. As shown in Figure 3(a), our model achieves the lowest average gap to the best
 444 method across all tasks, with narrow interquartile ranges, indicating stable performance. These
 445 results demonstrate that embedding-based approaches, when combined with architectural enhance-
 446 ments, can offer a robust and efficient alternative to heavyweight LLM-based rerankers.
 447

448 **Efficiency.** We also evaluate the inference speed of each method, measured as the number of
 449 queries processed per second on a single A100 GPU. As shown in Table 1, EBCAR achieves a
 450 throughput of 29.33 queries per second, substantially outperforming all reranking baselines in terms
 451 of efficiency, while maintaining strong ranking quality. While models such as monoBERT and
 452 monoT5 have comparable parameter sizes to EBCAR, they process each query-passage pair inde-
 453 pendently, requiring k separate forward passes for k candidate passages per query. This leads to
 454 slower inference, especially in the case of pairwise models like duoT5, which compare passages
 455 in pairs and further increase the computational burden. At the other extreme, large LLM-based
 456 rerankers such as ICR or RankGPT are significantly slower due to both their large model sizes and
 457 their need to process the full textual content of all candidate passages. Even when some models like
 458 FIRST and FirstMistral do not explicitly generate output sequences, e.g., listwise orders like [3]
 459 > [1] > [2], their long input contexts still cause substantial latency.
 460

461 In contrast, EBCAR operates entirely in the embedding space, allowing all candidate passages to be
 462 encoded once independently. The final selection is performed through lightweight alignment computa-
 463 tions, without the need for autoregressive generation or full-sequence processing. This design
 464 yields an order-of-magnitude speedup while maintaining strong performance, clearly positioning
 465 EBCAR on the Pareto frontier of ranking quality versus speed, as obviously shown in Figure 3(b).
 466

467 **Summary.** Together, these results highlight that EBCAR offers a highly favorable integration of
 468 competitive ranking quality as well as fast and scalable inference.
 469

470 Interestingly, we observe that monoBERT and monoT5 trained on ConTEB perform worse than
 471 Contriever or when trained on MS-MARCO. We hypothesize this stems from the fact that during
 472 training these pointwise models are forced to separate semantically similar passages from the gold
 473 passages while unable to utilize the document-wise context, which is the actual signal to distinguish
 474 the passages. This resulted in poor generalization. In contrast, EBCAR can leverage global context
 475 and structural signals across the candidate set, enabling more robust and context-aware ranking.
 476

477 4.5 ABLATION STUDIES

478 We analyze the contri-
 479 bution of key compo-
 480 nents in EBCAR via ab-
 481 lation studies. Remov-
 482 ing positional informa-
 483 tion (*w/o Pos*), which in-
 484 cludes document ID em-
 485 beddings and passage po-

486 Table 2: Ablation studies on two core components of EBCAR.

Method	MLDR	SQuAD	NarrQA	COVID	ESG	Football	Geog	Insur
w/o Pos	60.72	60.87	64.18	43.71	23.36	42.88	62.44	34.16
w/o Hybrid	74.55	47.52	66.32	42.93	34.44	41.93	60.34	36.00
w/o Both	43.46	40.13	51.80	29.63	15.77	5.28	43.70	2.88
EBCAR	75.26	71.62	73.21	59.80	37.20	80.19	81.30	40.74

487 position encodings, leads to notable performance degradation, particularly on datasets like Insurance,
 488 where positional reasoning and document structure are critical. Ablating the hybrid attention mech-
 489 anism (*w/o Hybrid*) also results in performance drops on several datasets such as SQuAD. Interest-
 490 ingly, *w/o Hybrid* outperforms *w/o Pos* on datasets such as MLDLR, NarrQA, and ESG, while the
 491 opposite trend is observed on SQuAD, COVID, and Football. These variations in direction reflect
 492 dataset-specific characteristics. Tasks that rely heavily on structural or positional cues (e.g., *Insur-*

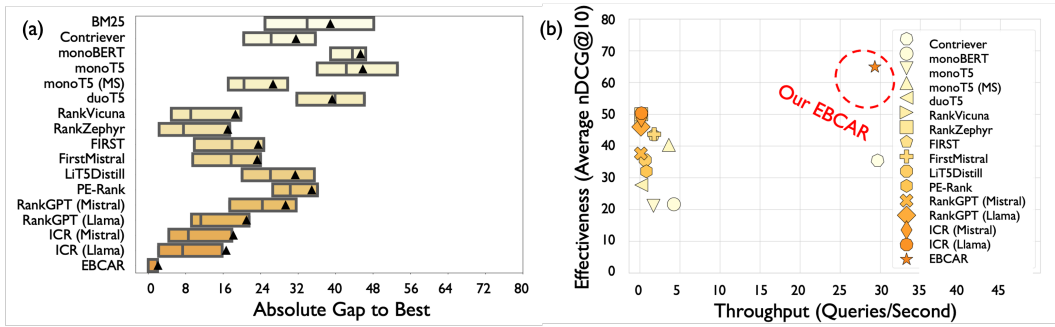


Figure 3: (a) For each method, we compute the gap in nDCG@10 from the best-performing method on each dataset. The boxes represent the interquartile range (25th to 75th percentile), vertical lines and black triangles indicate the median and mean, respectively. (b) An overall effectiveness-and-efficiency comparison across all methods. The effectiveness is measured by the average nDCG@10 across 8 test datasets. The efficiency is quantified by the throughput.

ance) are more affected by removing positional signals (w/o Pos), whereas datasets emphasizing semantic reconciliation across passages (e.g., *Football* and *Geography*) depend more on the hybrid attention for effective cross-passage reasoning (w/o Hybrid). This suggests that the two proposed components contribute complementarily to the overall performance of EBCAR. When both components are removed (w/o Both), performance deteriorates drastically across all datasets, underscoring the synergy between structural signals and the hybrid attention mechanism. These results validate the effectiveness of each component.

In Appendix A.5, we further analyze the hybrid attention mechanism through qualitative visualizations of its attention heatmaps. In Appendix A.6 and Appendix A.7, we evaluate EBCAR on datasets that do not emphasize cross-passage inference and the impact of retrieved candidate size.

4.6 ROBUSTNESS TO OTHER RETRIEVER

To examine the robustness of EBCAR to different embedding models, we replace the Contriever retriever and embeddings with E5 (Wang et al., 2024b), a stronger dense retriever. As shown by nDCG@10 scores, EBCAR maintains consistent performance improvements across datasets and further benefits from the stronger embedding space provided by E5. Specifically, the retriever-only E5 achieves 62.78 on MLDR, 55.86 on SQuAD, 67.12 on NarrQA, 33.74 on COVID, 15.38 on ESG, 6.05 on Football, 48.85 on Geography, and 4.02 on Insurance. When combined with EBCAR, the E5-based variant achieves 77.36 on MLDR, 72.68 on SQuAD, 75.04 on NarrQA, 61.07 on COVID, 36.88 on ESG, 80.64 on Football, 82.47 on Geography, and 41.24 on Insurance. These results confirm that EBCAR is retriever-agnostic and can seamlessly adapt to stronger embedding models while consistently improving overall retrieval quality.

5 CONCLUSION AND DISCUSSION

In this work, we introduce EBCAR, a novel embedding-based reranking framework designed to model context across multiple retrieved passages, by leveraging their structural signals and a hybrid attention mechanism. Extensive experiments on the ConTEB benchmark demonstrate that EBCAR outperforms strong baselines, especially on challenging datasets requiring entity disambiguation, co-reference resolution, and structural understanding.

540 REPRODUCIBILITY STATEMENT
541542 For reproducibility, we provide implementation details of our method in Section 4.3 and those of the
543 baseline methods in Appendix A.3. The full codebase will be released publicly upon acceptance of
544 this paper.

545

546

547

548

549

550

551

552

553

554

555

556

557

558

559

560

561

562

563

564

565

566

567

568

569

570

571

572

573

574

575

576

577

578

579

580

581

582

583

584

585

586

587

588

589

590

591

592

593

594 REFERENCES
595

596 596 Omar Adjali. Exploring retrieval augmented generation for real-world claim verification. In *Pro-
597 ceedings of the Seventh Fact Extraction and VERification Workshop (FEVER)*, pp. 113–117, Mi-
598 ami, Florida, USA, 2024. Association for Computational Linguistics.

599 599 Manoj Ghuhan Arivazhagan, Lan Liu, Peng Qi, Xinchi Chen, William Yang Wang, and Zhiheng
600 Huang. Hybrid hierarchical retrieval for open-domain question answering. In Anna Rogers,
601 Jordan Boyd-Graber, and Naoaki Okazaki (eds.), *Findings of the Association for Computational
602 Linguistics: ACL 2023*, pp. 10680–10689, Toronto, Canada, 2023. Association for Computational
603 Linguistics.

604 604 Payal Bajaj, Daniel Campos, Nick Craswell, Li Deng, Jianfeng Gao, Xiaodong Liu, Rangan Ma-
605 jumder, Andrew McNamara, Bhaskar Mitra, Tri Nguyen, Mir Rosenberg, Xia Song, Alina Stoica,
606 Saurabh Tiwary, and Tong Wang. Ms marco: A human generated machine reading comprehension
607 dataset, 2016.

608 608 Nicolas Boizard, Hippolyte Gisserot-Boukhlef, Duarte M. Alves, André Martins, Ayoub Hammal,
609 Caio Corro, Céline Hudelot, Emmanuel Malherbe, Etienne Malaboeuf, Fanny Jourdan, Gabriel
610 Hautreux, Jo ao Alves, Kevin El-Haddad, Manuel Faysse, Maxime Peyrard, Nuno M. Guerreiro,
611 Patrick Fernandes, Ricardo Rei, and Pierre Colombo. Eurobert: Scaling multilingual encoders for
612 european languages, 2025.

613 613 Shijie Chen, Bernal Jimenez Gutierrez, and Yu Su. Attention in large language models yields effi-
614 cient zero-shot re-rankers. In *The Thirteenth International Conference on Learning Representa-
615 tions*, 2025.

616 616 Zijian Chen, Ronak Pradeep, and Jimmy Lin. An early first reproduction and improvements to
single-token decoding for fast listwise reranking, 2024.

617 617 Jaeyoung Choe, Jihoon Kim, and Woohwan Jung. Hierarchical retrieval with evidence curation
618 for open-domain financial question answering on standardized documents. In *Findings of the
619 Association for Computational Linguistics: ACL 2025*, pp. 16663–16681, Vienna, Austria, 2025.
620 Association for Computational Linguistics. ISBN 979-8-89176-256-5.

621 621 Max Conti, Manuel Faysse, Gautier Viaud, Antoine Bosselut, Céline Hudelot, and Pierre Colombo.
622 Context is gold to find the gold passage: Evaluating and training contextual document embed-
623 dings, 2025.

624 624 Nick Craswell, Bhaskar Mitra, Emine Yilmaz, Daniel Campos, and Ellen M. Voorhees. Overview
625 of the trec 2019 deep learning track, 2020.

626 626 Nick Craswell, Bhaskar Mitra, Emine Yilmaz, and Daniel Campos. Overview of the trec 2020 deep
627 learning track, 2021.

628 628 Gabriel de Souza P. Moreira, Ronay Ak, Benedikt Schifferer, Mengyao Xu, Radek Osmulski, and
629 Even Oldridge. Enhancing q&a text retrieval with ranking models: Benchmarking, fine-tuning
630 and deploying rerankers for rag, 2024.

631 631 Aaron Grattafiori et al. The llama 3 herd of models, 2024.

632 632 Revanth Gangi Reddy, JaeHyeok Doo, Yifei Xu, Md Arafat Sultan, Deevya Swain, Avirup Sil, and
633 Heng Ji. FIRST: Faster improved listwise reranking with single token decoding. In *Proceedings
634 of the 2024 Conference on Empirical Methods in Natural Language Processing*, pp. 8642–8652,
635 Miami, Florida, USA, 2024. Association for Computational Linguistics.

636 636 Michael Glass, Gaetano Rossiello, Md Faisal Mahbub Chowdhury, Ankita Naik, Pengshan Cai, and
637 Alfio Gliozzo. Re2G: Retrieve, rerank, generate. In Marine Carpuat, Marie-Catherine de Marn-
638 effe, and Ivan Vladimir Meza Ruiz (eds.), *Proceedings of the 2022 Conference of the North Amer-
639 ican Chapter of the Association for Computational Linguistics: Human Language Technologies*,
640 pp. 2701–2715, Seattle, United States, 2022. Association for Computational Linguistics.

641 641 Michael Günther, Isabelle Mohr, Daniel James Williams, Bo Wang, and Han Xiao. Late chunking:
642 Contextual chunk embeddings using long-context embedding models, 2025.

648 Qiushi Huang, Shuai Fu, Xubo Liu, Wenwu Wang, Tom Ko, Yu Zhang, and Lilian Tang. Learning
 649 retrieval augmentation for personalized dialogue generation. In Houda Bouamor, Juan Pino, and
 650 Kalika Bali (eds.), *Proceedings of the 2023 Conference on Empirical Methods in Natural Lan-*
 651 *guage Processing*, pp. 2523–2540, Singapore, 2023. Association for Computational Linguistics.
 652

653 Gautier Izacard, Mathilde Caron, Lucas Hosseini, Sebastian Riedel, Piotr Bojanowski, Armand
 654 Joulin, and Edouard Grave. Unsupervised dense information retrieval with contrastive learning,
 655 2021.

656 Mathew Jacob, Erik Lindgren, Matei Zaharia, Michael Carbin, Omar Khattab, and Andrew Drozdov.
 657 Drowning in documents: Consequences of scaling reranker inference, 2024.

658 Albert Q. Jiang, Alexandre Sablayrolles, Arthur Mensch, Chris Bamford, Devendra Singh Chap-
 659 lot, Diego de las Casas, Florian Bressand, Gianna Lengyel, Guillaume Lample, Lucile Saulnier,
 660 Lélio Renard Lavaud, Marie-Anne Lachaux, Pierre Stock, Teven Le Scao, Thibaut Lavril, Thomas
 661 Wang, Timothée Lacroix, and William El Sayed. Mistral 7b, 2023.

662 Ziyang Jiang, Xueguang Ma, and Wenhui Chen. Longrag: Enhancing retrieval-augmented generation
 663 with long-context llms, 2024.

664 Diederik P. Kingma and Jimmy Ba. Adam: A method for stochastic optimization. In Yoshua Bengio
 665 and Yann LeCun (eds.), *3rd International Conference on Learning Representations, ICLR 2015,*
 666 *San Diego, CA, USA, May 7-9, 2015, Conference Track Proceedings*, 2015.

667 Patrick S. H. Lewis, Ethan Perez, Aleksandra Piktus, Fabio Petroni, Vladimir Karpukhin, Naman
 668 Goyal, Heinrich Küttler, Mike Lewis, Wen-tau Yih, Tim Rocktäschel, Sebastian Riedel, and
 669 Douwe Kiela. Retrieval-augmented generation for knowledge-intensive NLP tasks. In Hugo
 670 Larochelle, Marc'Aurelio Ranzato, Raia Hadsell, Maria-Florina Balcan, and Hsuan-Tien Lin
 671 (eds.), *Advances in Neural Information Processing Systems 33: Annual Conference on Neural*
 672 *Information Processing Systems 2020, NeurIPS 2020, December 6-12, 2020, virtual*, 2020.

673 Qi Liu, Bo Wang, Nan Wang, and Jiaxin Mao. Leveraging passage embeddings for efficient listwise
 674 reranking with large language models. In *The Web Conference 2025*, 2025.

675 Sean MacAvaney, Andrew Yates, Sergey Feldman, Doug Downey, Arman Cohan, and Nazli Go-
 676 harian. Simplified data wrangling with ir_datasets. In Fernando Diaz, Chirag Shah, Torsten Suel,
 677 Pablo Castells, Rosie Jones, and Tetsuya Sakai (eds.), *SIGIR '21: The 44th International ACM SI-*
 678 *GIR Conference on Research and Development in Information Retrieval, Virtual Event, Canada,*
 679 *July 11-15, 2021*, pp. 2429–2436. Acm, 2021.

680 Yuning Mao, Pengcheng He, Xiaodong Liu, Yelong Shen, Jianfeng Gao, Jiawei Han, and Weizhu
 681 Chen. Generation-augmented retrieval for open-domain question answering. In Chengqing Zong,
 682 Fei Xia, Wenjie Li, and Roberto Navigli (eds.), *Proceedings of the 59th Annual Meeting of the*
 683 *Association for Computational Linguistics and the 11th International Joint Conference on Natural*
 684 *Language Processing (Volume 1: Long Papers)*, pp. 4089–4100, Online, 2021. Association for
 685 Computational Linguistics.

686 Rodrigo Nogueira, Wei Yang, Kyunghyun Cho, and Jimmy Lin. Multi-stage document ranking with
 687 bert, 2019.

688 Rodrigo Nogueira, Zhiying Jiang, Ronak Pradeep, and Jimmy Lin. Document ranking with a pre-
 689 trained sequence-to-sequence model. In Trevor Cohn, Yulan He, and Yang Liu (eds.), *Findings*
 690 *of the Association for Computational Linguistics: EMNLP 2020*, pp. 708–718, Online, 2020.
 691 Association for Computational Linguistics.

692 Ronak Pradeep, Rodrigo Nogueira, and Jimmy Lin. The expando-mono-duo design pattern for text
 693 ranking with pretrained sequence-to-sequence models, 2021.

694 Ronak Pradeep, Sahel Sharifmoghaddam, and Jimmy Lin. Rankvicuna: Zero-shot listwise docu-
 695 ment reranking with open-source large language models, 2023a.

696 Ronak Pradeep, Sahel Sharifmoghaddam, and Jimmy Lin. Rankzephyr: Effective and robust zero-
 697 shot listwise reranking is a breeze!, 2023b.

702 Renyi Qu, Ruixuan Tu, and Forrest Bao. Is semantic chunking worth the computational cost?, 2024.
 703

704 Sahel Sharifmoghaddam, Ronak Pradeep, Andre Slavescu, Ryan Nguyen, Andrew Xu, Zijian
 705 Chen, Yilin Zhang, Yidi Chen, Jasper Xian, and Jimmy Lin. Rankilm: A python package for
 706 reranking with llms. In *Proceedings of the 48th International ACM SIGIR Conference on Re-*
 707 *search and Development in Information Retrieval*, Sigir '25, pp. 3681–3690, New York, NY,
 708 USA, 2025. Association for Computing Machinery. ISBN 9798400715921.

709 Weiwei Sun, Lingyong Yan, Xinyu Ma, Shuaiqiang Wang, Pengjie Ren, Zhumin Chen, Dawei Yin,
 710 and Zhaochun Ren. Is ChatGPT good at search? investigating large language models as re-
 711 ranking agents. In Houda Bouamor, Juan Pino, and Kalika Bali (eds.), *Proceedings of the 2023*
 712 *Conference on Empirical Methods in Natural Language Processing*, pp. 14918–14937, Singapore,
 713 2023. Association for Computational Linguistics.

714 Manveer Singh Tamber, Ronak Pradeep, and Jimmy Lin. Scaling down, litting up: Efficient zero-
 715 shot listwise reranking with seq2seq encoder-decoder models, 2023.

716 Nandan Thakur, Nils Reimers, Andreas Rücklé, Abhishek Srivastava, and Iryna Gurevych. Beir: A
 717 heterogenous benchmark for zero-shot evaluation of information retrieval models, 2021.

718 Nandan Thakur, Jimmy Lin, Sam Havens, Michael Carbin, Omar Khattab, and Andrew Drozdov.
 719 Freshstack: Building realistic benchmarks for evaluating retrieval on technical documents, 2025.

720 Aaron van den Oord, Yazhe Li, and Oriol Vinyals. Representation learning with contrastive predic-
 721 tive coding, 2018.

722 Hongru Wang, Wenyu Huang, Yang Deng, Rui Wang, Zeyzhong Wang, Yufei Wang, Fei Mi, Jeff Z.
 723 Pan, and Kam-Fai Wong. Unims-rag: A unified multi-source retrieval-augmented generation for
 724 personalized dialogue systems, 2024a.

725 Liang Wang, Nan Yang, Xiaolong Huang, Binxing Jiao, Linjun Yang, Dixin Jiang, Rangan Ma-
 726 jumder, and Furu Wei. Text embeddings by weakly-supervised contrastive pre-training, 2024b.
 727 URL <https://arxiv.org/abs/2212.03533>.

728 Benjamin Warner, Antoine Chaffin, Benjamin Clavié, Orion Weller, Oskar Hallström, Said
 729 Taghadouini, Alexis Gallagher, Raja Biswas, Faisal Ladhak, Tom Aarsen, Nathan Cooper, Griffin
 730 Adams, Jeremy Howard, and Iacopo Poli. Smarter, better, faster, longer: A modern bidirectional
 731 encoder for fast, memory efficient, and long context finetuning and inference, 2024.

732 Shangyu Wu, Ying Xiong, Yufei Cui, Haolun Wu, Can Chen, Ye Yuan, Lianming Huang, Xue
 733 Liu, Tei-Wei Kuo, Nan Guan, and Chun Jason Xue. Retrieval-augmented generation for natural
 734 language processing: A survey, 2024.

735 Peng Xu, Wei Ping, Xianchao Wu, Lawrence McAfee, Chen Zhu, Zihan Liu, Sandeep Subramanian,
 736 Evelina Bakhturina, Mohammad Shoeybi, and Bryan Catanzaro. Retrieval meets long context
 737 large language models. In *The Twelfth International Conference on Learning Representations*,
 738 *ICLR 2024, Vienna, Austria, May 7-11, 2024*. OpenReview.net, 2024a.

739 Zhentao Xu, Mark Jerome Cruz, Matthew Guevara, Tie Wang, Manasi Deshpande, Xiaofeng Wang,
 740 and Zheng Li. Retrieval-augmented generation with knowledge graphs for customer service ques-
 741 tion answering. In Grace Hui Yang, Hongning Wang, Sam Han, Claudia Hauff, Guido Zuccon,
 742 and Yi Zhang (eds.), *Proceedings of the 47th International ACM SIGIR Conference on Research*
 743 *and Development in Information Retrieval, SIGIR 2024, Washington DC, USA, July 14-18, 2024*,
 744 pp. 2905–2909. Acm, 2024b.

745 Zhenrui Yue, Huimin Zeng, Lanyu Shang, Yifan Liu, Yang Zhang, and Dong Wang. Retrieval
 746 augmented fact verification by synthesizing contrastive arguments. In *Proceedings of the 62nd*
 747 *Annual Meeting of the Association for Computational Linguistics (Volume 1: Long Papers)*, pp.
 748 10331–10343, Bangkok, Thailand, 2024. Association for Computational Linguistics.

749 Xin Zhang, Yanzhao Zhang, Dingkun Long, Wen Xie, Ziqi Dai, Jialong Tang, Huan Lin, Baosong
 750 Yang, Pengjun Xie, Fei Huang, Meishan Zhang, Wenjie Li, and Min Zhang. mGTE: Generalized
 751 long-context text representation and reranking models for multilingual text retrieval. In *Proceed-
 752 ings of the 2024 Conference on Empirical Methods in Natural Language Processing: Industry*
 753 *Track*, pp. 1393–1412, Miami, Florida, US, 2024. Association for Computational Linguistics.

756 Yang Zhou, Hongyi Liu, Zhuoming Chen, Yuandong Tian, and Beidi Chen. Gsm-infinite: How do
757 your llms behave over infinitely increasing context length and reasoning complexity?, 2025.
758

759 Dawei Zhu, Liang Wang, Nan Yang, Yifan Song, Wenhao Wu, Furu Wei, and Sujian Li. LongEm-
760 bed: Extending embedding models for long context retrieval. In *Proceedings of the 2024 Confer-
761 ence on Empirical Methods in Natural Language Processing*, pp. 802–816, Miami, Florida, USA,
762 2024. Association for Computational Linguistics.

763
764
765
766
767
768
769
770
771
772
773
774
775
776
777
778
779
780
781
782
783
784
785
786
787
788
789
790
791
792
793
794
795
796
797
798
799
800
801
802
803
804
805
806
807
808
809

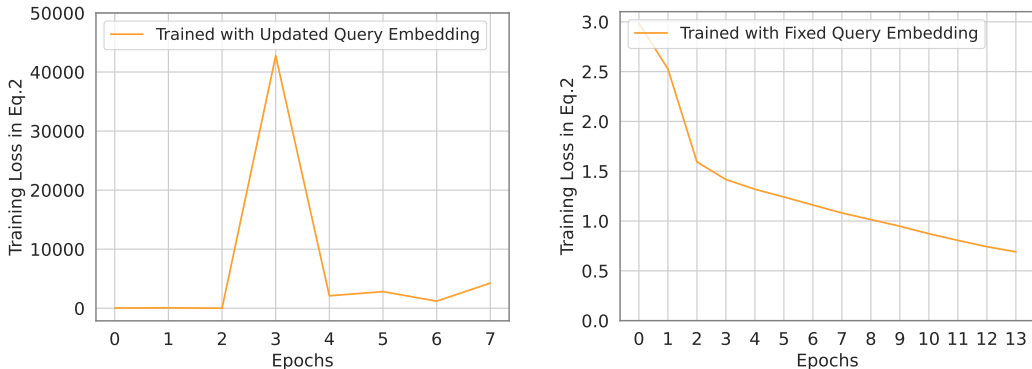


Figure 4: Training loss comparison between using an **updated query embedding** (left) and a **fixed query embedding** (right) in Eq. 2. Updating the query embedding leads to large and unstable loss spikes, while keeping it fixed produces smooth and monotonic convergence. This supports our design choice to use a fixed query embedding.

LLM USAGE

We employed large language models exclusively to assist with polishing the writing of this paper. Specifically, LLMs were used to refine wording and verify grammar for clarity and readability. No aspects of method design, implementation, or experimental analysis involved LLM assistance.

A APPENDIX

A.1 TRAINING WITH UPDATED QUERY EMBEDDING

To examine the effect of fixing the query embedding in the contrastive objective in Eq. 2, we compare two variants of EBCAR: one that uses the fixed input query embedding q , and another that uses the updated query representation produced by the encoder to compute the loss. As shown in Figure 4, training becomes highly unstable when the query embedding is updated. Loss values oscillate drastically and occasionally explode after a few epochs. In contrast, the fixed-query variant converges smoothly and yields stable optimization. We attribute this instability to *context drift*, where the query representation becomes entangled with passage-specific context, thus breaking its role as a consistent semantic anchor across candidate sets. These results empirically validate our design choice of using the unmodified query embedding in Eq. 2.

A.2 SUPPLEMENTAL MRR@10 RESULTS

We provide full MRR@10 results in Table 3. The overall trends are consistent with our nDCG@10 results. EBCAR achieves the highest average score across all datasets. Notably, EBCAR excels on datasets such as Football, Geog, and Insurance, demonstrating its strong ability in handling tasks that benefit from structured passage representation and alignment. These findings reinforce the motivations behind EBCAR and validate its robustness across varying cross-passage reasoning challenges.

A.3 SUPPLEMENTAL IMPLEMENTATION DETAILS

For monoBERT and monoT5 trained on ConTEB, we implement these two models from scratch. For training, we use the Adam optimizer (Kingma & Ba, 2015) with a fixed learning rate of 2×10^{-5} and 5×10^{-5} , respectively, as suggested in their original implementation details (Nogueira et al., 2019; 2020). These models are trained for up to 20 epochs, with early stopping based on validation loss using a patience of 5 epochs. We set the batch size to 32. All other baseline implementations are based on public code releases: monoT5 (MS-MARCO), duoT5, RankVicuna, RankZephyr, First-Mistral, and LiT5Distill are from the RankLLM library (Sharifmoghaddam et al., 2025)². Following ICR (Chen et al., 2025), we use open-source models Mistral (Jiang et al., 2023)³ and Llama-

²https://github.com/castorini/rank_llm

³<https://huggingface.co/mistralai/Mistral-7B-Instruct-v0.2>

864
 865 Table 3: MRR@10 across datasets. **Orange** denotes in-distribution tests, and **Green** denotes out-
 866 of-distribution tests. Throughput is the number of queries processed per second on a single A100
 867 GPU. The best and second best results are **bolded** and underlined, respectively.

Method	Training	Size	MLDR	SQuAD	NarrQA	COVID	ESG	Football	Geog	Insur	Avg	Throughput
BM25	-	-	61.35	42.90	36.18	37.35	8.56	3.72	23.46	0.00	26.69	263.16
Contriever	-	-	52.00	49.94	60.10	25.25	11.63	4.48	37.87	1.72	30.37	29.67
monoBERT (base)	ConTEB Train	110M	31.50	20.00	25.87	14.63	7.96	2.73	21.96	2.31	15.87	4.24
monoT5 (base)	ConTEB Train	223M	16.97	<u>13.26</u>	30.39	17.87	6.31	4.36	28.07	3.35	15.07	1.69
monoT5 (base)	MS-MARCO	223M	66.59	64.91	51.44	38.39	14.83	8.63	47.82	1.35	36.75	3.61
duoT5 (base)	MS-MARCO	223M	35.25	66.89	16.14	14.88	10.75	7.68	42.23	1.69	24.44	0.18
RankVicuna	MS-MARCO	7B	77.13	64.45	77.13	50.62	19.69	10.71	67.71	3.21	46.33	0.17
RankZephyr	MS-MARCO	7B	<u>80.77</u>	67.54	79.27	52.41	23.67	<u>10.95</u>	70.13	2.88	48.45	0.17
FIRST	MS-MARCO	7B	71.43	59.16	76.10	38.73	17.39	7.08	57.20	2.41	41.19	1.73
FirstMistral	MS-MARCO	7B	70.93	60.03	76.24	39.04	17.64	6.95	58.37	2.83	41.50	1.78
LiT5Distil	MS-MARCO	248M	52.10	50.18	60.10	25.46	12.01	4.53	38.15	1.75	30.54	0.66
PE-Rank	MS-MARCO	8B	41.32	35.93	39.34	25.42	16.04	4.48	35.34	0.52	24.80	0.81
RankGPT (Mistral)	-	7B	58.93	52.20	61.97	27.80	10.07	6.44	44.34	1.81	32.95	0.12
RankGPT (Llama)	-	8B	73.45	57.64	70.70	45.35	17.23	10.40	68.40	4.13	43.41	0.13
ICR (Mistral)	-	7B	77.04	65.61	78.63	<u>52.53</u>	23.21	9.76	69.27	2.85	47.36	0.18
ICR (Llama)	-	8B	82.93	67.83	<u>79.18</u>	53.64	25.38	10.18	<u>71.33</u>	2.87	49.17	0.19
EBCAR (ours)	ConTEB Train	126M	68.34	64.50	67.44	51.44	26.04	74.73	75.61	20.54	56.08	29.33

884
 885 3.1 (et al., 2024)⁴ for the RankGPT method, instead of GPT3.5/4 due to cost constraints. FIRST⁵,
 886 PE-Rank⁶, RankGPT and ICR⁷ follow their respective original implementations. All experiments
 887 are run on a single A100 GPU.

888 A.4 EXAMPLES OF FOOTBALL AND INSURANCE

890 Example 1 (Football).

891 **Query:** What was Andrew Henry Robertson's first goal for Hull City?

892 **Gold passage:** Despite the departure of several other first-team players, he chose to remain at
 893 City. His inaugural goal for the club was scored on 3 November 2015 in an away match against
 894 Brentford, where he initiated the scoring in a 2–0 victory that placed Hull at the top of the
 895 Championship table on goal difference. He participated in the 2016 Championship play-off final
 896 against Sheffield Wednesday, which Hull won 1–0 to achieve promotion to the Premier League.
 897 However, the team lasted only one season in the top division before being relegated again.

898
 899 All pronouns in this dataset are anonymized, so identifying that "he" refers to "Andrew Henry
 900 Robertson" requires reasoning across multiple passages mentioning the player and the club.
 901 EBCAR's hybrid attention enables such cross-passage coreference resolution effectively.

903 Example 2 (Insurance).

904 **Query:** What is the amount of (Re)insurance GWP in million in Austria?

905 **Gold passage:** { 'General data': '— Amounts — Share total EEA —
 906 — Population (in 1000) — 8,979 — 2.00% —
 907 — (Re)insurance GWP (in million) — 20,815.873 — 1.5% —
 908 — Number of (re)insurance undertakings — 33 — 1.9% —
 909 — Number of registered insurance intermediaries — 17,999 — 2.1% —' }

910
 911 Without positional or structural cues, it is difficult to associate this numerical information with the
 912 correct country (Austria), which only appears in the section title. EBCAR's positional encodings
 913 provide this structural grounding, allowing accurate passage ranking.

914
 915 ⁴<https://huggingface.co/meta-llama/Llama-3.1-8B-Instruct>

916 ⁵<https://github.com/gangiswag/llm-reranker>

917 ⁶https://github.com/liuqi6777/pe_rank

918 ⁷<https://github.com/OSU-NLP-Group/In-Context-Reranking>

918 Table 4: nDCG@10 of selected baselines and EBCAR on TREC21, TREC22.
919

920 Method	921 Training	922 Size	923 TREC2021	924 TREC2022	925 Average	926 Throughput
927 BM25	928 -	929 -	930 54.10	931 48.66	932 51.38	933 263.16
934 Contriever	935 -	936 -	937 64.19	938 61.36	939 62.78	940 29.67
941 monoT5	942 ConTEB Train	943 223M	944 52.57	945 46.66	946 49.62	947 1.69
948 monoT5	949 MS-MARCO	950 223M	951 85.04	952 76.92	953 80.98	954 3.61
956 RankZephyr	957 MS-MARCO	958 7B	959 88.05	960 79.87	961 83.96	962 0.17
964 ICR (Llama)	965 -	966 8B	967 75.28	968 67.47	969 71.38	970 0.19
973 EBCAR (ours)	974 ConTEB Train	975 126M	976 72.77	977 66.65	978 69.71	979 29.33

980 **A.5 HYBRID ATTENTION ANALYSIS**

981 To examine how the hybrid attention mechanism routes information, we conduct a qualitative study
982 across all datasets. For each dataset, we randomly sample 20 test queries and, for every example,
983 render an aggregated attention heatmap averaged over heads. We focus our analysis on the **final**
984 **layer (Layer 15)** where the model’s decision is consolidated. Figure 6 shows the **shared full attention**
985 at Layer 15. Although weights vary across cells, attention is broadly distributed across passages,
986 indicating global context exchange among all candidates. In contrast, Figure 7 shows the **dedicated**
987 **masked attention** at Layer 15: information flow is sharply concentrated within passages that origi-
988 nate from the same document (block-diagonal patterns) and between the query and those passages.
989 *While the figures present one representative case, we observe the same qualitative pattern consis-
990 tently across the 20 sampled examples in every dataset:* the shared full attention supports global
991 cross-passage reconciliation, whereas the dedicated masked attention strengthens intra-document
992 consolidation. This matches EBCAR’s design intent and explains the complementary gains seen in
993 the ablations.

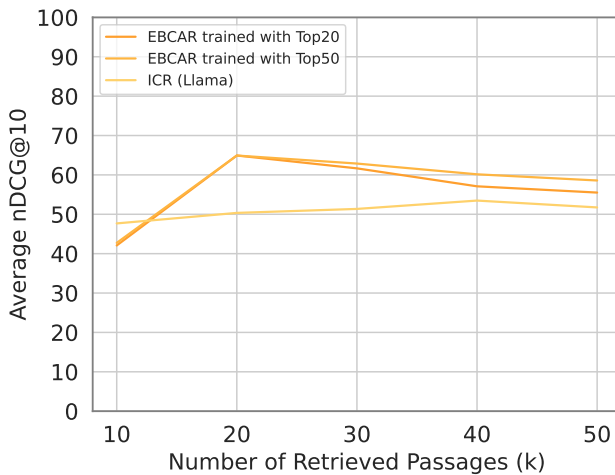
994 **A.6 PERFORMANCE ON MS-MARCO V2**

995 To further evaluate the generalization ability of EBCAR, we compare it against selected rerankers on
996 the MS-MARCO v2 dataset, using test queries from TREC 2021 and 2022. We select ICR (Llama)
997 because it is the most recent and best-performing baseline on the ConTEB Test set, and thus serves
998 as a strong comparator in this evaluation. RankZephyr and monoT5 are selected because they are
999 the best-performing methods among LLM-supervised distillation methods and point-wise methods,
1000 respectively.

1001 Compared to MS-MARCO v1, version 2 provides additional structural annotations such as docu-
1002 ment IDs and passage spans, making it a suitable testbed for evaluating EBCAR’s ability to leverage
1003 structural signals (Bajaj et al., 2016). We utilize the `ir_datasets` library (MacAvaney et al.,
1004 2021) to access the judged queries from the TREC Deep Learning Tracks (2021 and 2022).

1005 As shown in Table 4, EBCAR achieves comparable ranking performance to ICR (Llama), despite
1006 being significantly smaller in model size. Moreover, EBCAR exhibits a dramatically higher through-
1007 put, highlighting its practical advantage in scenarios that demand both efficiency and effectiveness.

1008 While EBCAR performs competitively against ICR, it does not surpass monoT5 (MS-MARCO)
1009 or RankZephyr, both of which are pretrained and fine-tuned directly on MS-MARCO v1. We hy-
1010 pothesize two main reasons for this gap: (1) MS-MARCO v2 contains multiple golden passages
1011 per query. However, EBCAR is trained with the setting where there are only one golden passage
1012 among all candidate passages. This mismatch makes it harder for EBCAR to adapt to multi-relevant
1013 retrieval settings. (2) Both monoT5 (MS-MARCO) and RankZephyr are trained specifically on the
1014 MS-MARCO v1 dataset, which has overlaps with MS-MARCO v2 queries and documents, giving
1015 them an implicit domain advantage.

972 A.7 IMPACT OF RETRIEVED CANDIDATE SIZE
973
974990 Figure 5: Impact of retrieved candidate size.
991
992

993 In this section, we study how the performance of EBCAR varies as the number of retrieved can-
994 didate passages increases during inference. By default, EBCAR is trained with $k = 20$ passages,
995 which defines the positional range of its document ID embeddings and sinusoidal position encod-
996 ings. During inference, however, increasing k beyond this value may result in extrapolation issues
997 due to embedding mismatches or index overflows.

998 To study this issue, we train an additional variant of EBCAR using $k = 50$ passages and compare
999 its performance against the default $k = 20$ variant, as well as against ICR (Llama), across varying
1000 numbers of retrieved passages from 10 to 50.

1001 As shown in Figure 5, we observe that: **(i)** The default EBCAR (trained with Top20) degrades as k
1002 increases after $k = 20$, likely due to extrapolation effects from unseen positional indices. **(ii)** The
1003 EBCAR trained with Top50 exhibits more stable performance across larger k values and consistently
1004 outperforms EBCAR trained with Top20 variant beyond $k = 30$, validating our hypothesis about
1005 training-inference mismatch. **(iii)** Interestingly, both EBCAR variants exhibit a slight performance
1006 drop at large k , which aligns with prior findings (Jacob et al., 2024), where scaling up candidate size
1007 introduces noisy or distractive information that hampers reranking. **(iv)** Compared to ICR (Llama),
1008 both EBCAR variants outperform it across most k values. These results suggest that it is better to
1009 train the EBCAR model with larger size of candidate passages during the training phase to mitigate
1010 the extrapolation issue for inference.

1011
1012
1013
1014
1015
1016
1017
1018
1019
1020
1021
1022
1023
1024
1025

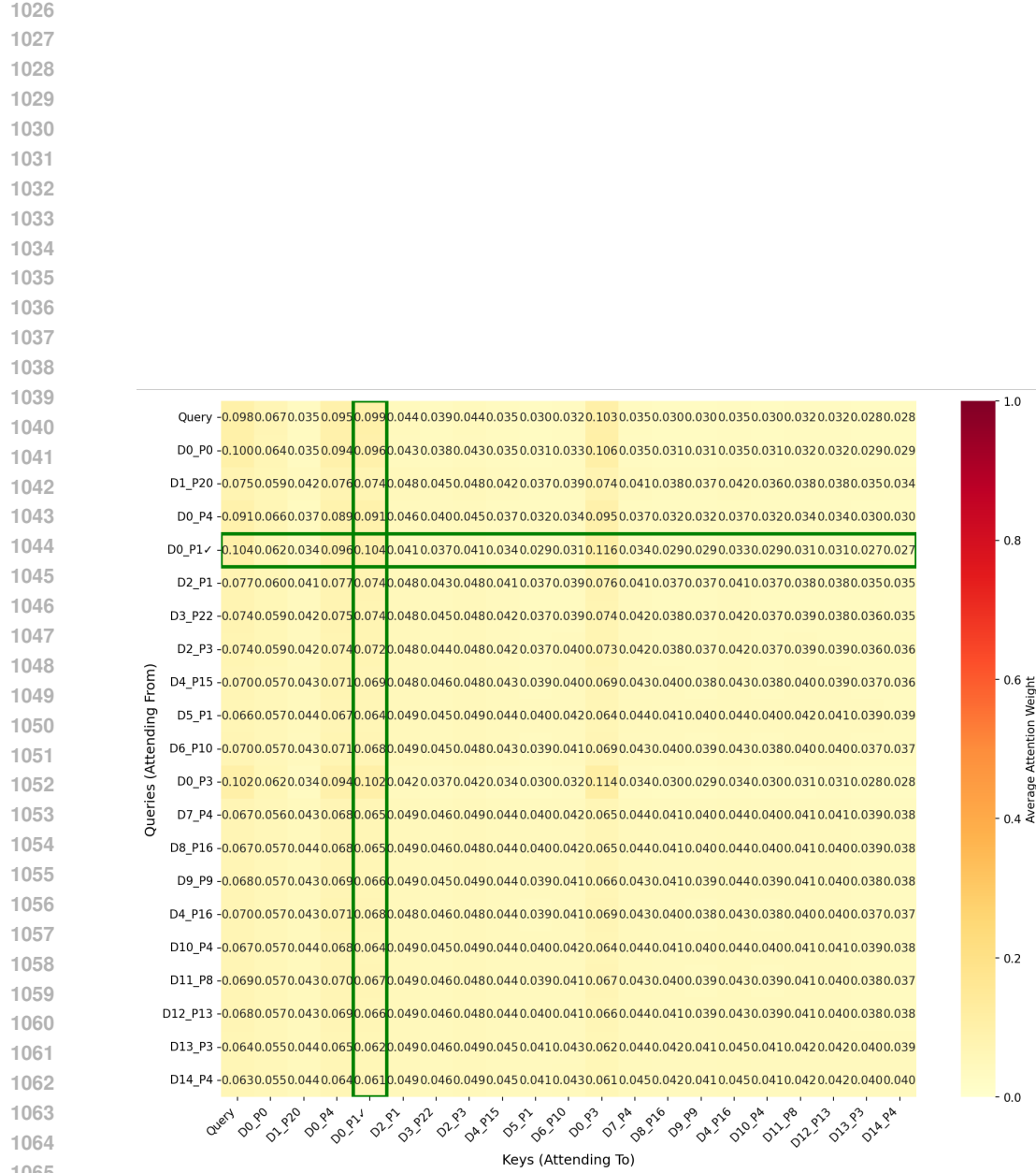


Figure 6: **Shared full attention at Layer 15**, averaged over all heads. The green box highlights the gold passage. Attention is more broadly distributed across passages, indicating global context exchange among all candidates.

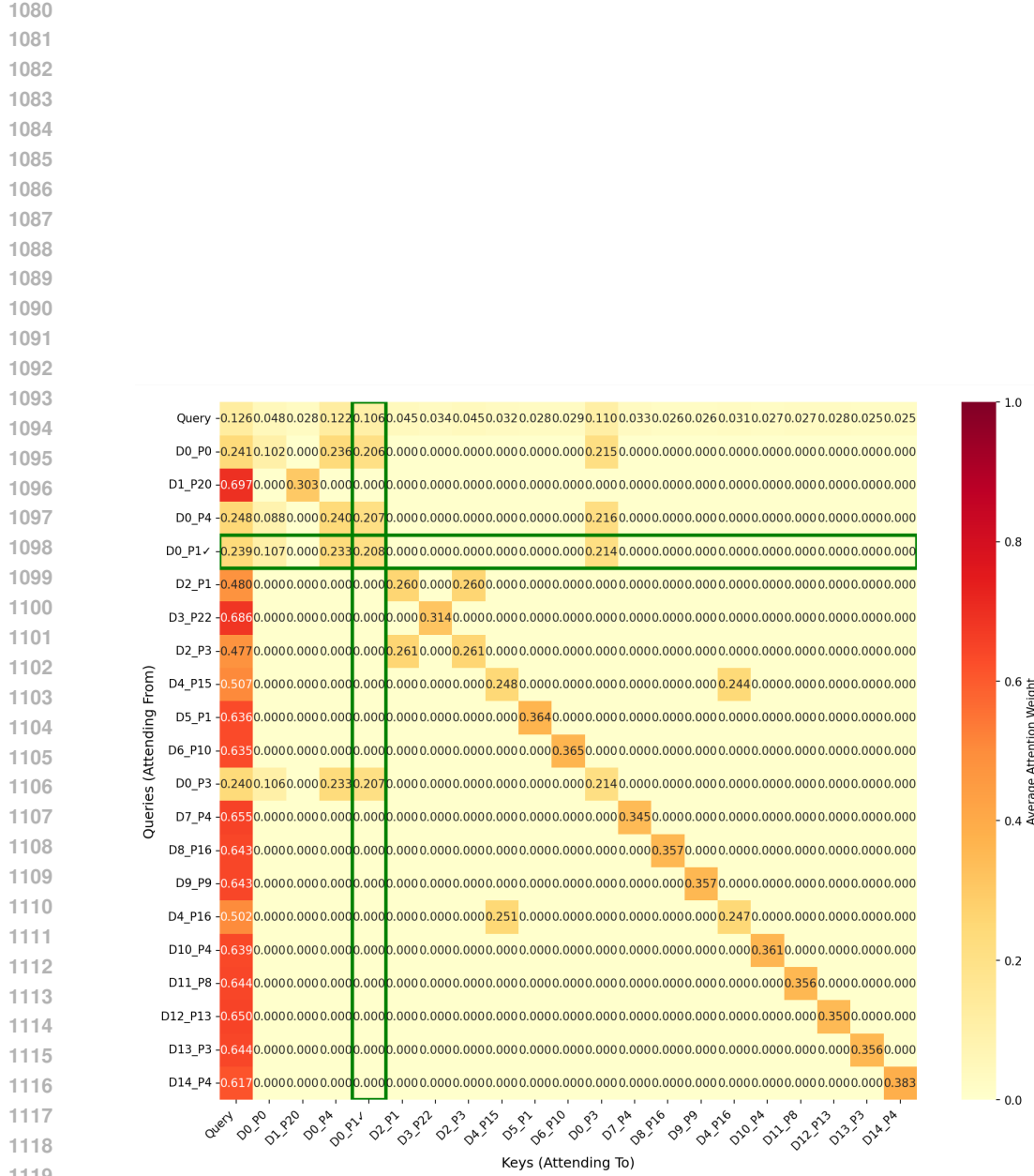


Figure 7: **Dedicated masked attention at Layer 15**, averaged over all heads. The green box highlights the gold passage. Attention concentrates within passages from the same document (block-diagonal structure) and between the query and those passages, reflecting document-aware locality.